Electronic Supplementary Material (ESI) for Journal of Materials Chemistry A.

Supporting Information for

'Antifouling' Porous Loofahs Sponge with Internal Microchannels as Solar Absorbers and Water Pumpers for Thermal Desalination

Chao Liu, Kevin Hong, Xiao Sun, Avi Natan, Pengcheng Luan, Yang Yang, Hongli Zhu *

Department of Mechanical and Industrial Engineering, Northeastern University, Boston, Massachusetts 02115, USA

***Corresponding author**: Dr. Hongli Zhu; **E-mail:** h.zhu@neu.edu;

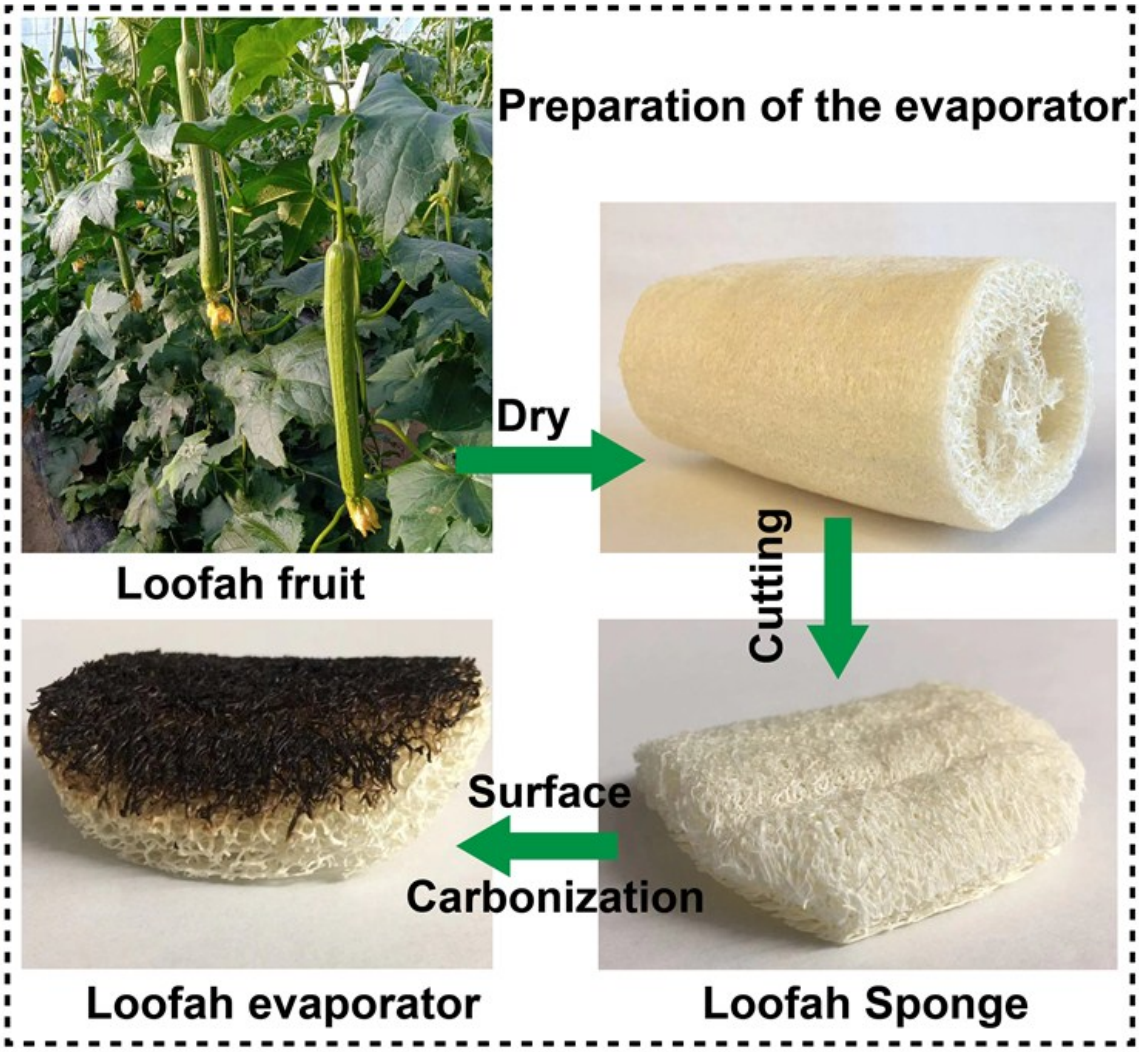

Figure S1. Photographs illustrating the fabrication of the loofah based evaporator from loofah fruit.

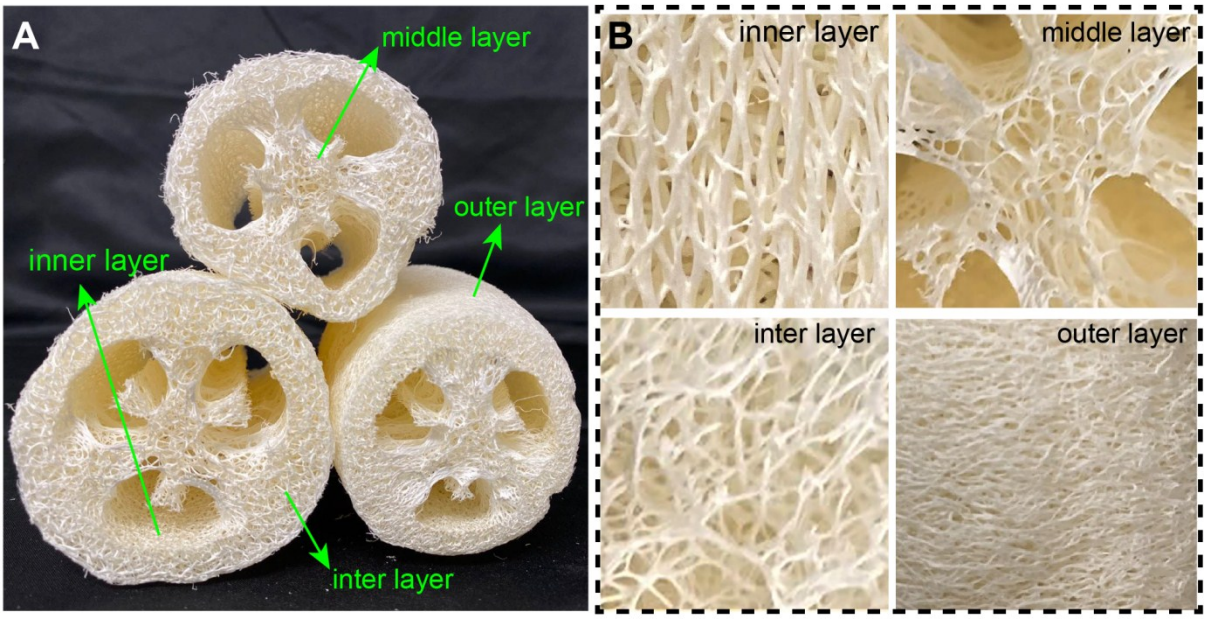

Figure S2. Photographs of (A) features of loofah sponges, (B) loofah sponge fiber bundles from four parts, which is composed of an outer, inter, middle, and inner layer.

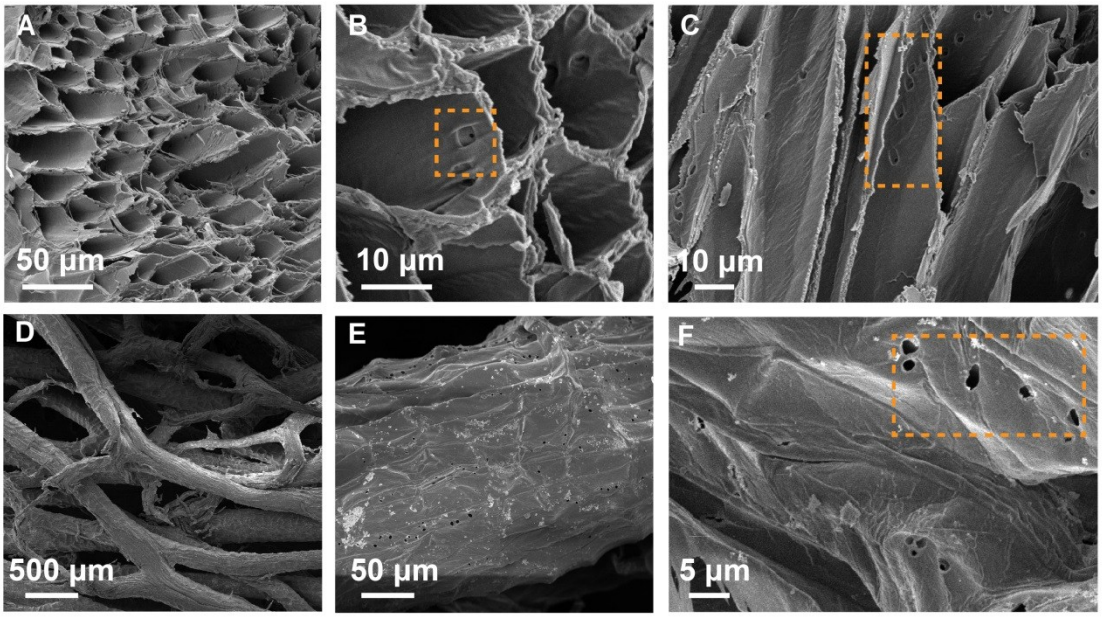

Figure S3. Morphology characterization of the loofah sponge. (A), (B), (C) SEM images show the micro-channels inside the loofah fiber, and there are also some small pores in these micro-channels, (D), (E), (F) SEM images show the pores structure of the surface of the loofah fiber at different magnifications. These unique porous structures play an essential role in the passage of salts and salt exchange.

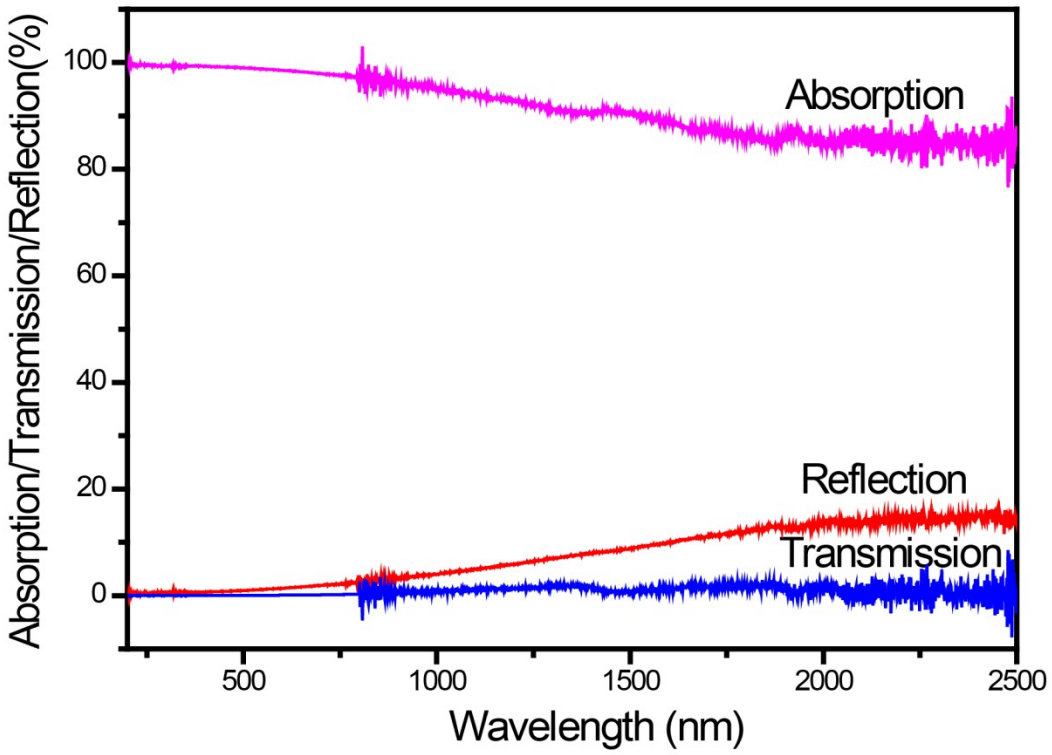

Figure S4. Absorption, reflection, and transmission spectra of loofah based evaporator in the wavelength range 200-2500 nm. The absorption spectrum is calculated from reflection and transmission spectra (A=1-R-T).

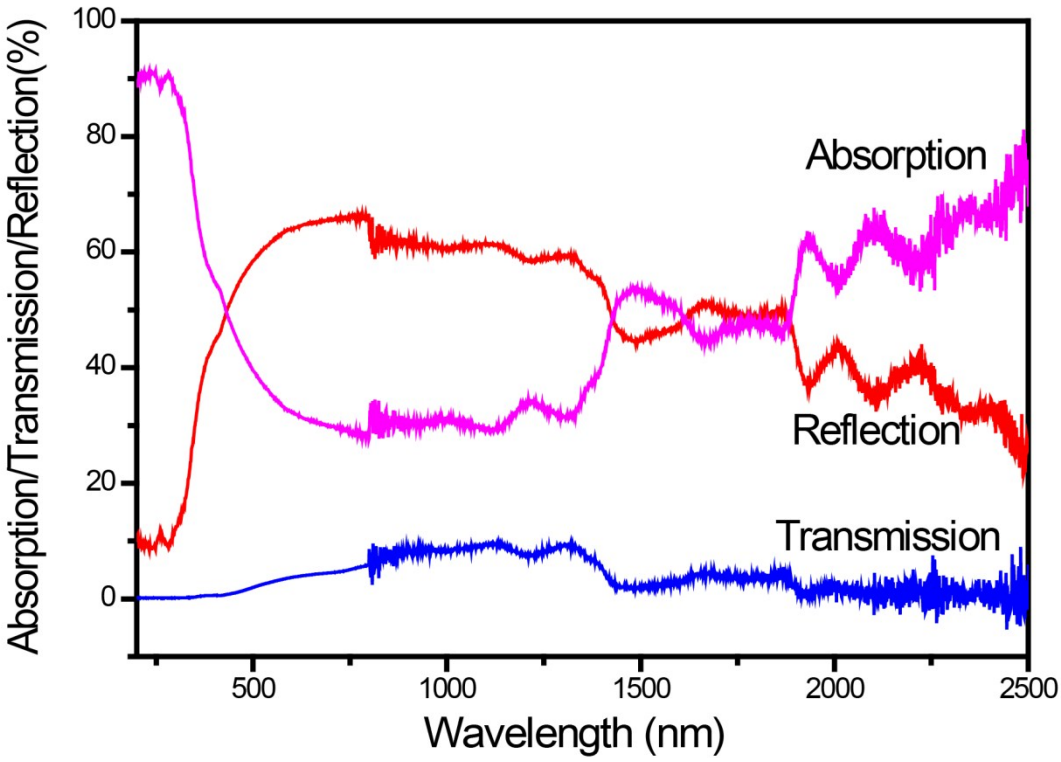

Figure S5. Absorption, reflection, and transmission spectra of natural loofah sponge in the wavelength range 200-2500 nm. The absorption spectrum is calculated from reflection and transmission spectra (A=1-R-T).

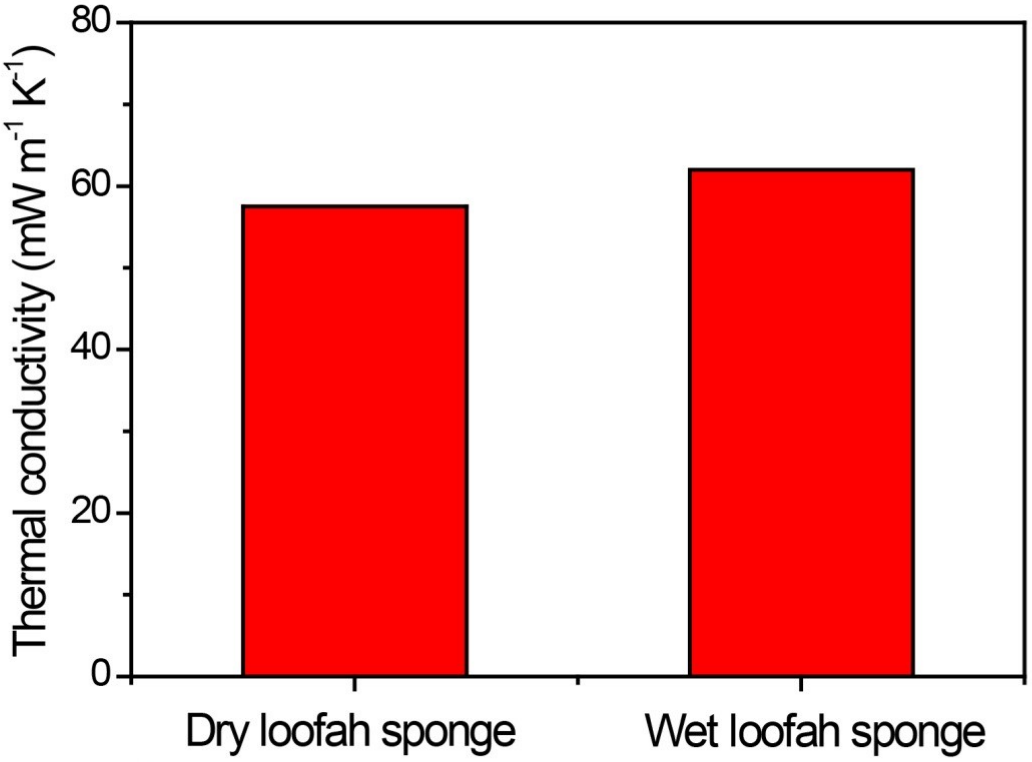

Figure S6. Thermal conductivity of dry loofah sponge and wet loofah sponge. The thermal conductivity of dry loofah sponge and wet loofah sponge is 57.5 mW m^{-1} K^{-1} and 62.0 mW m^{-1} K^{-1}, respectively.

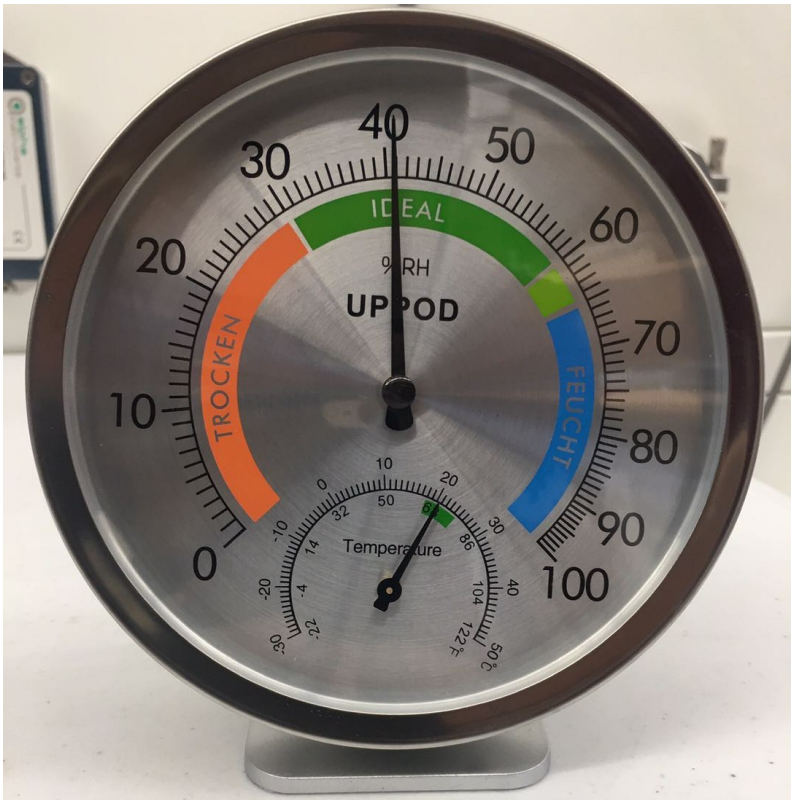

Figure S7. Digital images of the experimental temperature and humidity detector, which displays the indoor temperature of 20 ℃ and humidity of 40%.

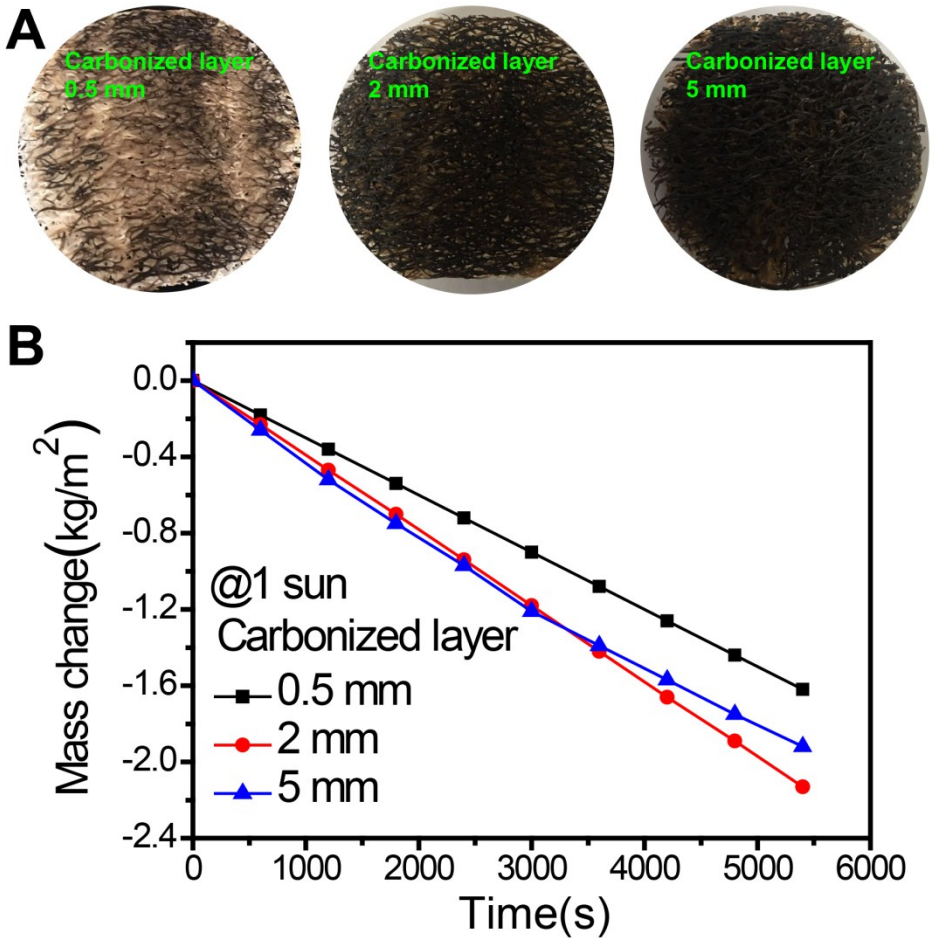

Figure S8. (A) Photograph of Loofah sponge evaporator with different thicknesses of the carbonized layer. (B) Mass changes of carbonized loofah sponge with different thicknesses of the carbonized layer under 1 Sun of illumination.

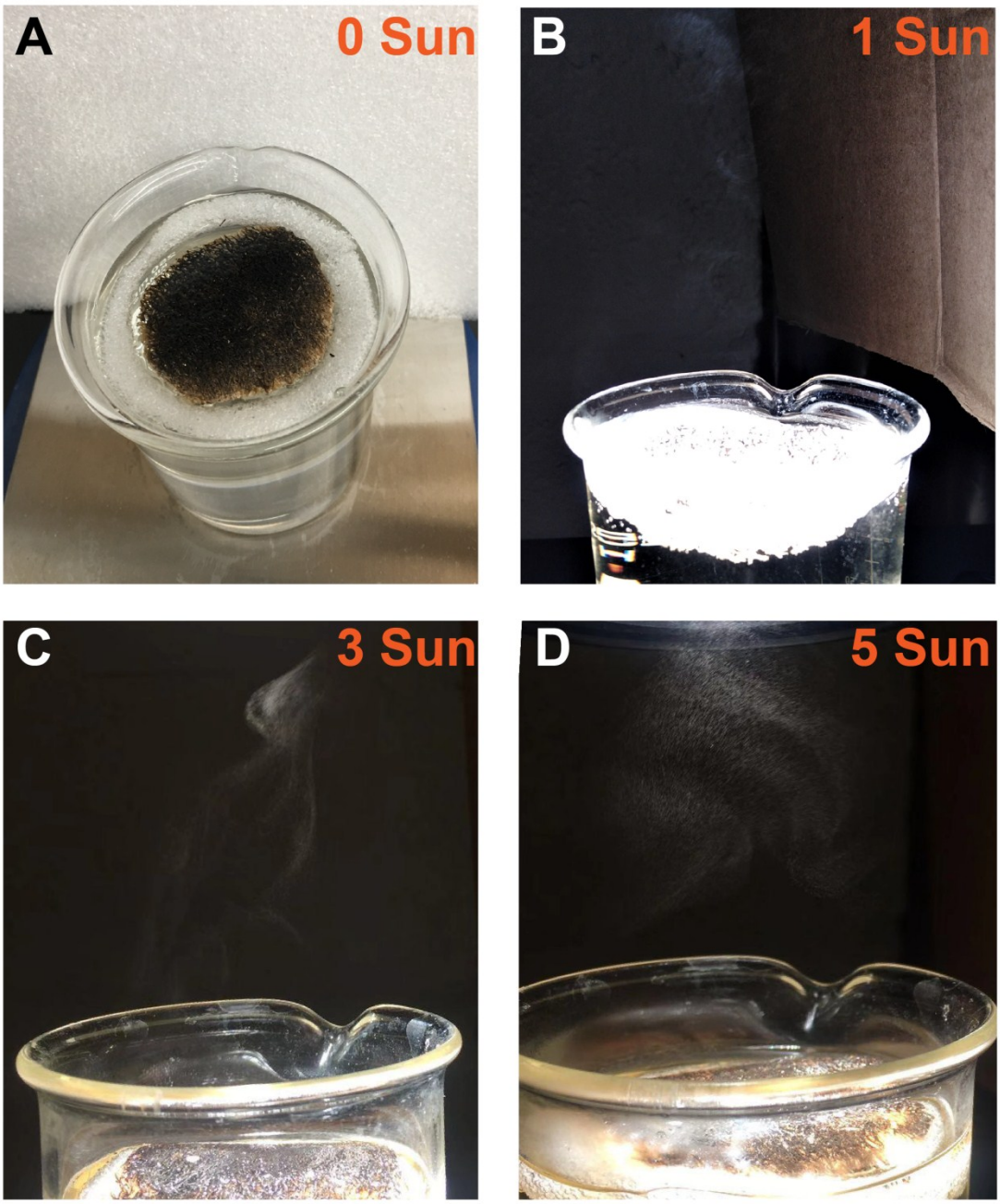

Figure S9. Digital images of the loofah based evaporator under different intensity illumination. (A) The loofah based evaporator can float on the water. (B), (C), (D) The steam coming from the carbonized loofah sponge surface at 1, 3, 5 sunlight intensities.

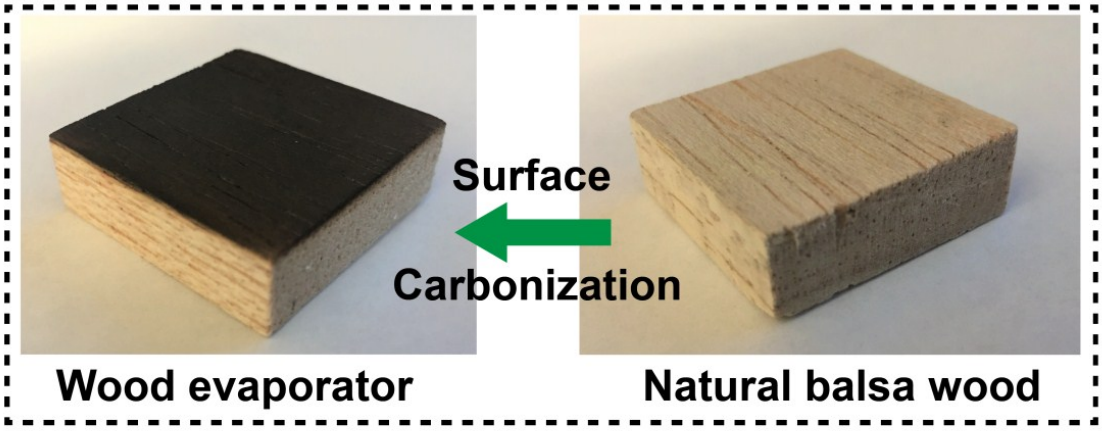

Figure S10. Photographs illustrating the fabrication of the wood evaporator.

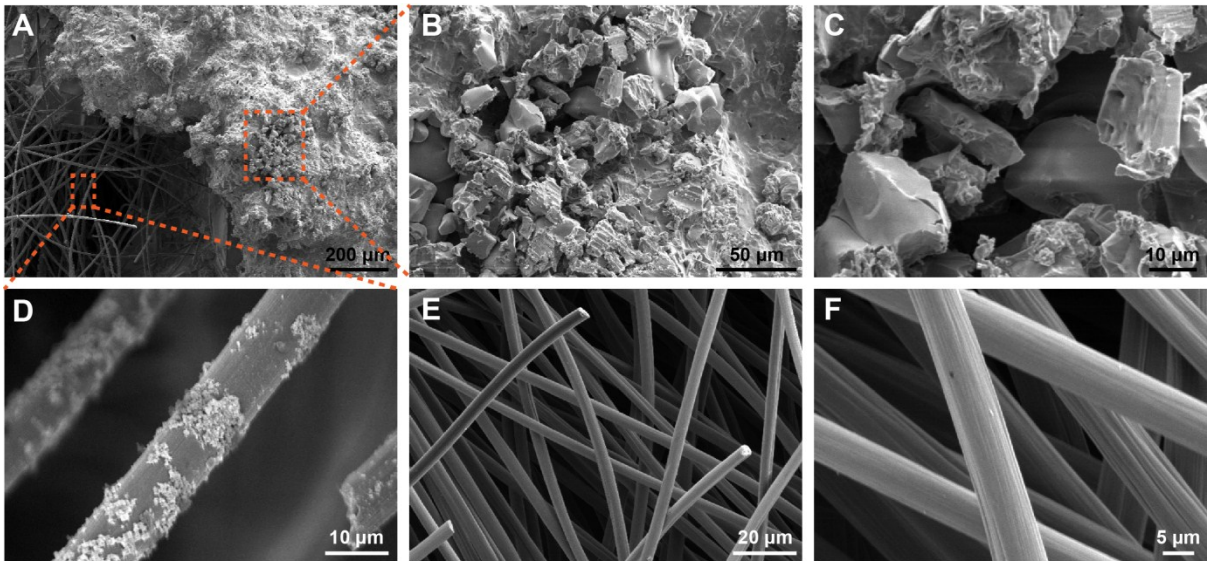

Figure S11. Morphology characterization of the carbon felt with salt accumulation after 10 h of 1 sun illumination in 20 wt. % seawater and pristine carbon felt. (A) SEM images show the precipitated salt on top of the carbon felt evaporator after 1 h. (B), (C) Magnified SEM images of A show salt accumulate on the carbon felt surface, these accumulated salts could severely affect the performance of the evaporator. (D) Salt crystals were observed starting from the carbon fiber and then gradually spreading over the carbon felt surface. (E), (F) SEM images show pristine carbon felt fiber at different magnifications.

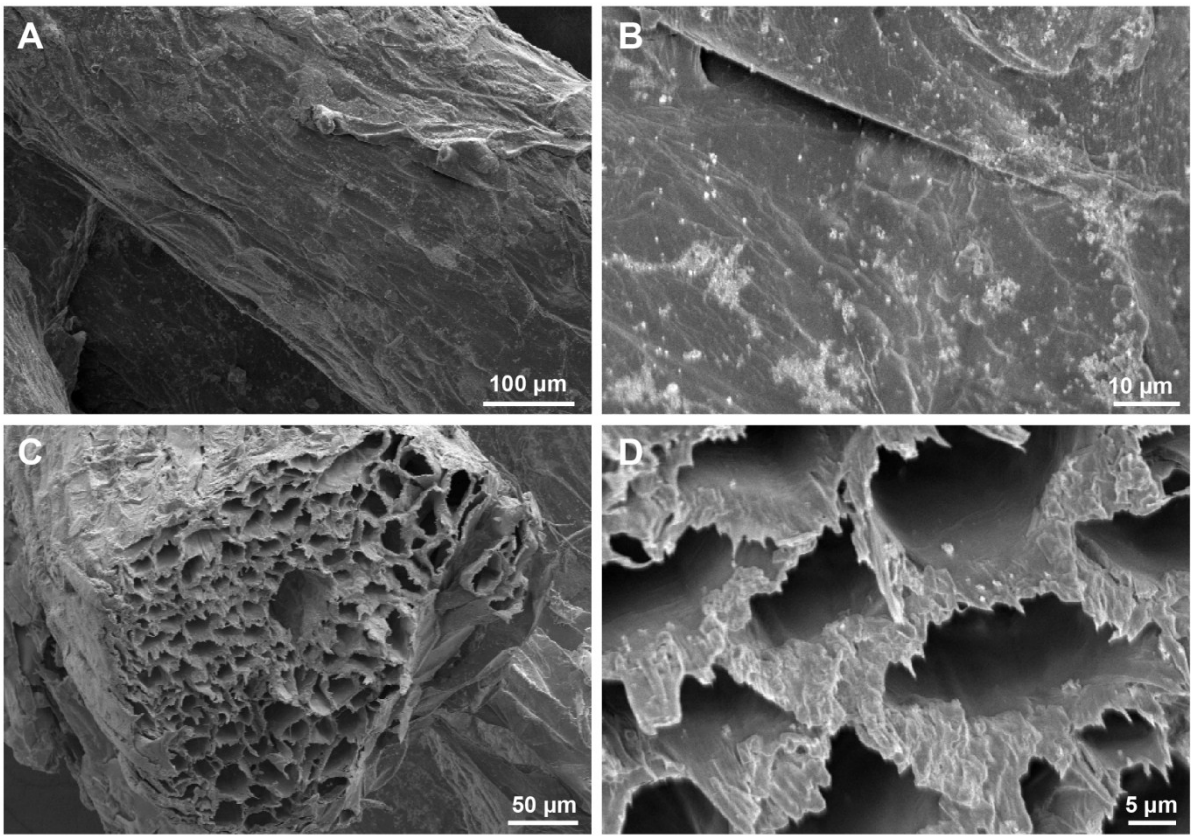

Figure S12. Morphology characterization of loofah sponge evaporator after 10 h of 1 sun illumination in 20 wt. % seawater. (A), (B) SEM images show the surface of the loofah fiber at different magnifications after desalination. (C), (D) SEM images show the internal microchannels of the loofah fiber at different magnifications after desalination. There was no obvious salt accumulation on the loofah fiber surface and internal microchannels.

Figure S13. Digital images of the PU sponge coated with a carbon black material. A collapse in the center of the PU material due to oxidative degradation appeared.

Energy loss analysis

The energy losses of the evaporator with an exposed area of 19.6 cm^2 under one sun irradiation is calculated as an example. The evaporator is fixed in white polystyrene (PS) foam framework to prevent the heat loss of the bulk solution from conduction and convection during test. The localized thermal energy at loofah based evaporator via photo-thermal conversion can be divided into five parts: energy consumption by water evaporator, loss of reflection on evaporator surface, heat radiation loss, heat conduction loss and heat convection loss. The detailed calculation of heat loss is analyzed below.

Evaporator surface reflection loss.

Considering the optical absorption of loofah based evaporator is about 95.4 %, the reflect heat loss should be about 4.6 %.

Radiation loss

The radiation loss of the evaporator is calculated by the Steafan-Boltzmann equation, as below,

$$\Phi = A\varepsilon\sigma(T_1^4 - T_2^4) \quad (1)$$

$$\text{Radiation loss} = \frac{\Phi}{Ac_{opt}q_i} = \frac{\varepsilon\sigma(T_1^4 - T_2^4)}{c_{opt}q_i} \quad (2)$$

Where Φ is the heat flux, ε is the emissivity of the absorbing surface (0.95), A represents the exposed area, σ is the Stefan-Boltzmann constant which is 5.67×10^{-8}J m^{-2} s^{-1} K^{-4}, T_1 is the surface temperature of loofah based evaporator (38.7 ℃).T_2 is the adjacent environment temperature (33.3 ℃). The radiation heat loss is 3.4% for the evaporator under 1 sun.

Conduction

Although PS foam are set as to prevent the heat loss of the bulk solution from conduction and convection, a portion heat loss conducted to bulk water might be occur via the loofah fiber path. The conduction loss is calculated based on the bulk water absorption heat Q as follows,

$Q=Cm\Delta T$ (3)

Conduction loss=$\frac{Q}{Ac_{opt}q_i \Delta t}=\frac{Cm \Delta T}{Ac_{opt}q_i \Delta t}$ (4)

Where Q represents the heat flux, C represents the specific heat capacity of water (4.2 kJ ℃$^{-1}$ kg^{-1}), m is the bulk water used in the experiment (100g), ΔT is the temperature change of the bulk water during the Δt (0.5 ℃ after 1 h). The conduction heat loss is 3.0 % in this experiment.

Convection

The convection loss is calculated based on the Newton's Law of Cooling as below,

$\Psi=\xi A\Delta T$ (5)

Convection loss= $\frac{\Psi}{Ac_{opt}q_i}=\frac{\xi \Delta T}{c_{opt}q_i}$ (6)

Where Ψ is the heat flux, ξ is the convection heat transfer coefficient (2.24 J m^{-2} s^{-1} K^{-1}), $^1\Delta T$ is the temperature difference between the surface temperature of the evaporator (38.7℃) and the adjacent environment temperature (33.3℃). The convective heat loss is 1.2% in this experiment.

In summary, the total heat loss for the loofah based evaporator under 1 sun is about 12.2%. Therefore the total energy consumption of the five parts is about 87.8%, which is in good agreement with the experimental photo-thermal conversion efficiency 89.9%.

Table S1. Steam generation performance of our loofah based evaporator compared to other steam generation devices under one sun illumination.

Materials	Evaporator rate under 1 sun ($kg\ m^{-2}\ h^{-1}$)	Efficiency (%)	Ref.
Graphite film	1.01	62.7%	R1[2]
F-wood/CNTs	0.95	65%	R2[3]
F-wood	1.05	72%	R3[4]
CNF/CNT aerogel	1.11	76.3%	R4[5]
Carbon Felt	1.22	79.4%	R5[6]
CNF membrane	1.32	82%	R6[7]
CB/GO	1.27	87.5%	R7[8]
Graphene oxide film	1.14	89.2%	R8[9]
Wood-PDA	1.04	87%	R9[10]
C-L-Wood	1.08	74%	R10[11]
Carbonized Loofah sponge	**1.42**	**89.9%**	**Our work**

References

1. Y. Li, T. Gao, Z. Yang, C. Chen, W. Luo, J. Song, E. Hitz, C. Jia, Y. Zhou and B. Liu, *Advanced materials*, 2017, **29**, 1700981.
2. S. MohammadáSajadi and S. HiáWang, *Journal of Materials Chemistry A*, 2017, **5**, 15227-15234.
3. C. Chen, Y. Li, J. Song, Z. Yang, Y. Kuang, E. Hitz, C. Jia, A. Gong, F. Jiang and J. Zhu, *Advanced materials*, 2017, **29**, 1701756.
4. G. Xue, K. Liu, Q. Chen, P. Yang, J. Li, T. Ding, J. Duan, B. Qi and J. Zhou, *ACS applied materials & interfaces*, 2017, **9**, 15052-15057.
5. F. Jiang, H. Liu, Y. Li, Y. Kuang, X. Xu, C. Chen, H. Huang, C. Jia, X. Zhao and E. Hitz, *ACS applied materials & interfaces*, 2017, **10**, 1104-1112.
6. H. Li, Y. He, Y. Hu and X. Wang, *ACS applied materials & interfaces*, 2018, **10**, 9362-9368.
7. Y. Wang, L. Zhang and P. Wang, *ACS Sustainable Chemistry & Engineering*, 2016, **4**, 1223-1230.
8. Y. Li, T. Gao, Z. Yang, C. Chen, Y. Kuang, J. Song, C. Jia, E. M. Hitz, B. Yang and L. Hu, *Nano Energy*, 2017, **41**, 201-209.
9. A. Guo, X. Ming, Y. Fu, G. Wang and X. Wang, *ACS applied materials & interfaces*, 2017, **9**, 29958-29964.
10. X. Wu, G. Y. Chen, W. Zhang, X. Liu and H. Xu, *Advanced Sustainable Systems*, 2017, **1**, 1700046.
11. H. Liu, C. Chen, G. Chen, Y. Kuang, X. Zhao, J. Song, C. Jia, X. Xu, E. Hitz and H. Xie, *Advanced Energy Materials*, 2018, **8**, 1701616.